

Electronic and magnetic properties of Lu and LuH₂

Shunda Zhang,^{1,*} Jiachang Bi,^{1,*} Ruyi Zhang,^{1,*} Peiyi Li,¹ Fugang Qi,¹ Zhiyang Wei,¹ and Yanwei Cao^{1,2,†}

¹*Ningbo Institute of Materials Technology and Engineering, Chinese Academy of Sciences, Ningbo 315201, China*

²*Center of Materials Science and Optoelectronics Engineering,*

University of Chinese Academy of Sciences, Beijing 100049, China

(Dated: March 21, 2023)

Clarifying the electronic and magnetic properties of lutetium, lutetium dihydride, and lutetium oxide is very helpful to understand the emergent phenomena in lutetium-based compounds (such as room-temperature superconductivity). However, this kind of study is still scarce at present. Here, we report on the electronic and magnetic properties of lutetium metals, lutetium dihydride powders, and lutetium oxide powders. Crystal structures and chemical compositions of these samples were characterized by X-ray diffraction and X-ray photoemission spectroscopy, respectively. Electrical transport measurements show that the resistance of lutetium has a linear behavior depending on temperature, whereas the resistance of lutetium dihydride powders is independent of temperature. More interestingly, paramagnetism-ferromagnetism-spin glass transitions were observed at near 240 and 200 K, respectively, in lutetium metals. Our work uncovered the complex magnetic properties of Lu-based compounds.

arXiv:2303.11063v1 [cond-mat.mtrl-sci] 20 Mar 2023

* These authors contributed equally to this work

† ywcao@nimte.ac.cn

I. INTRODUCTION

Due to the discovery of room-temperature superconductivity in nitrogen-doped lutetium (Lu) hydrides, the study of Lu-based compounds attracts a great deal of attention very recently [1–5]. Theoretical predication of high-temperature superconductivity in Lu hydrides (~ 273 K at the pressure 100 GPa in LuH_6) has been reported in the year 2020 [6, 7]. Experimental observation of superconductivity (with the critical temperature $T_C \sim 15$ K at the pressure 128 GPa) was realized in LuH_3 in 2021 [8, 9]. Then, the superconductivity critical temperature was increased to 71 K at the pressure 218 GPa in the compound Lu_4H_{23} [2]. However, whether near-ambient superconductivity can exist in Lu-based compounds is still an open question [1–5].

Besides the superconductivity, several other intriguing properties were also reported in Lu-based compounds such as high electrical conductivity and strong spin-orbit coupling in lutetium monoxide LuO [10], phase transformations in the Lu metal and LuH_3 [11, 12], ultrawide bandgap (5.5-5.9 eV) and luminescence in Lu_2O_3 [13, 14]. The element Lu with electron configuration $4f^{14}5d^16s^2$ is the last one of 14 rare-earth elements. Generally, the valence states of Lu can be Lu^0 , Lu^{2+} , and Lu^{3+} at ambient. Interestingly, superconductivity was observed in the compounds with Lu^0 or Lu^{2+} or Lu^{3+} valence state [1, 8]. Clarifying the electronic and magnetic properties of lutetium-based compounds is very helpful to understand the emergent phenomena. However, this kind of study is still scarce at present [15, 16].

To address the above, we investigated the structural, electronic, and magnetic properties of Lu^0 metals, $(\text{Lu}^{2+})\text{H}_2$ powders, and $(\text{Lu}^{3+}_2)\text{H}_3$ powders with X-ray diffractometer (XRD), X-ray photoemission spectroscopy (XPS), electrical transport, and

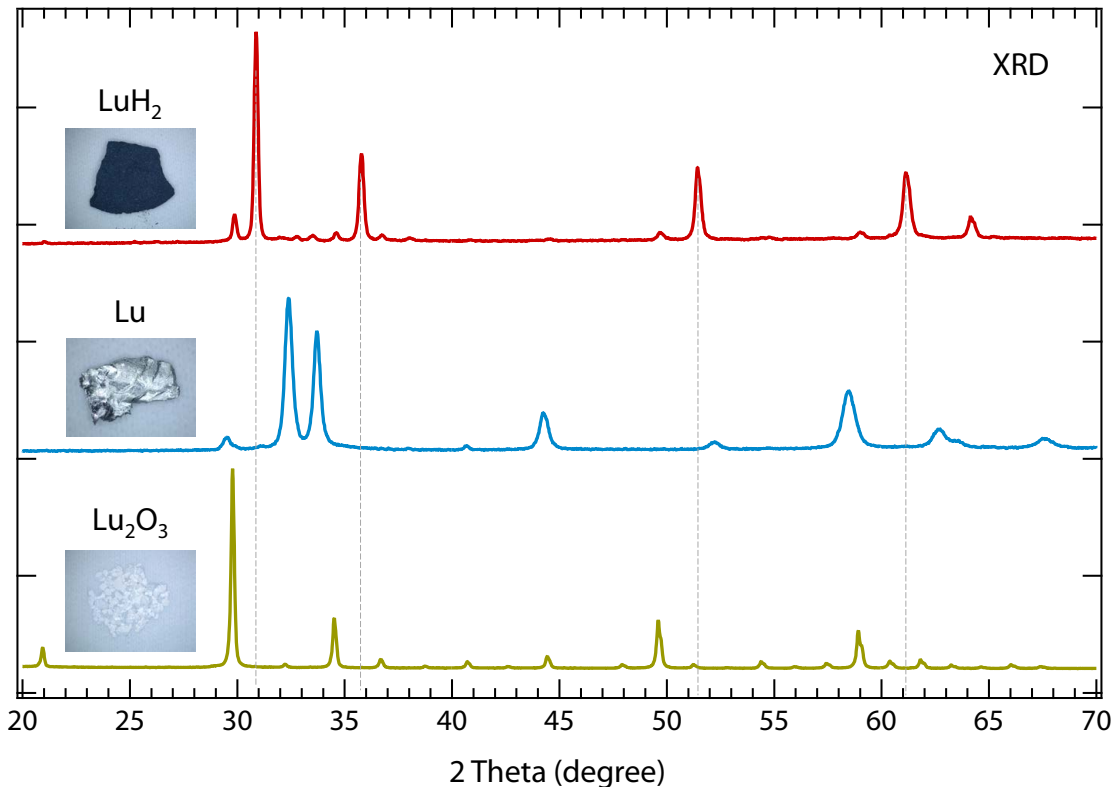


FIG. 1. XRD data of Lu metals, LuH_2 powders, and Lu_2O_3 powders at room temperature. The insets show photographs of three samples. The colours of Lu metals, LuH_2 powders (compressed), and Lu_2O_3 powders are silvery white, dark blue, and white, respectively.

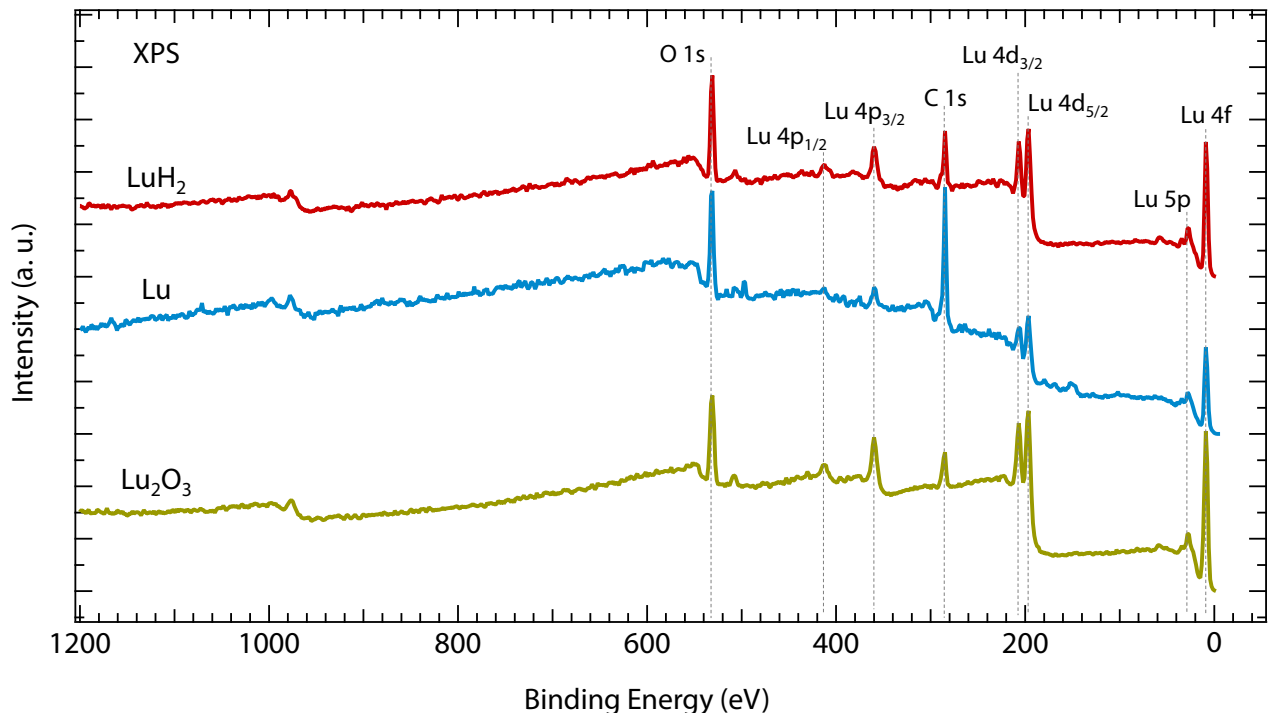


FIG. 2. XPS spectra of Lu metals, LuH₂ powders, and Lu₂O₃ powders from 0 to 1200 eV at room temperature.

a magnetometer with the superconducting quantum interference device (SQUID). It is revealed that both LuH₂ and Lu show complex magnetic transitions.

II. EXPERIMENTS

All samples (Lu polycrystalline metals, LuH₂ powders, and Lu₂O₃ powders, see the insets in Fig.1) studied in this work are commercial. The Lu polycrystalline metals (silvery white) were ordered from Griem Advanced Materials (China), whereas the dark blue LuH₂ powders (misabeled as “Lu”, purity of 99.9%, analogous to the samples reported in ref. 4) and white Lu₂O₃ powders were purchased from Macklin (China). The $2\theta - \omega$ scans on three samples were carried out by a powder XRD (Bruker D8 Discover) with the Cu K _{α} source. To characterize the chemical compositions of samples, XPS (monochromatic Al K _{α} radiation, $h\nu = 1486.6$ eV, Kratos AXIS Supra) was performed at room temperature. The electrical properties were measured from 300 to 2 K by Physical Property Measurement System (PPMS) in a van der Pauw geometry (DynaCool, Quantum Design). To measure the electrical transport of LuH₂, it is noted that the LuH₂ powders were compressed into several tablets at room temperature. Temperature-dependent magnetic properties were characterized by a SQUID magnetometer from the temperature 300 to 2 K.

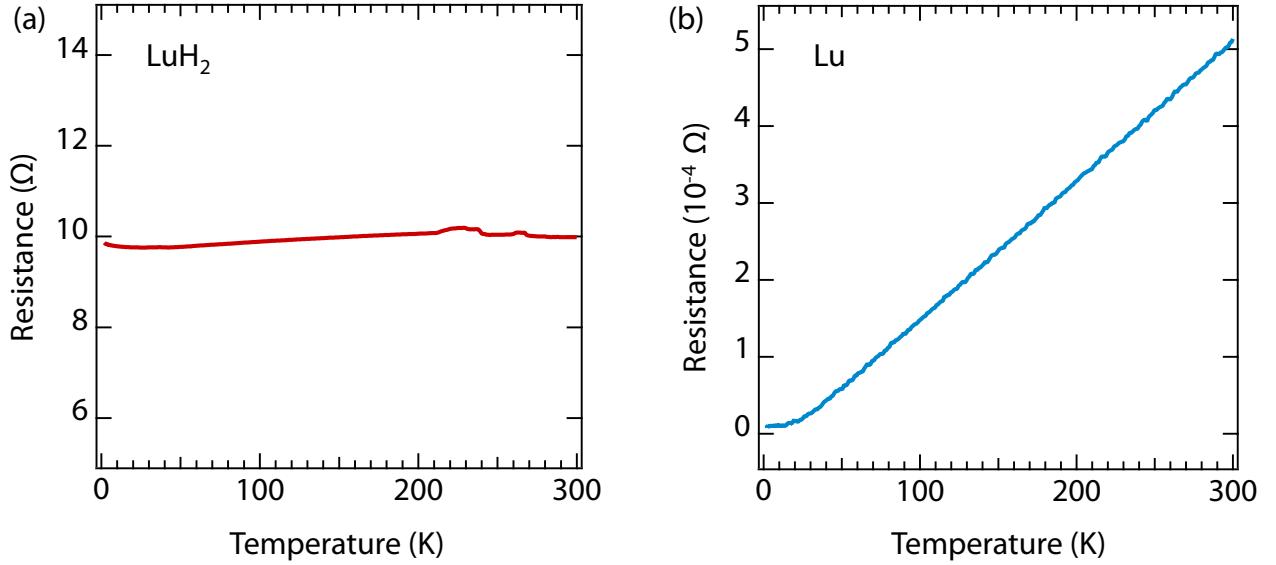


FIG. 3. Temperature-dependent resistances of (a) LuH₂ powders (compressed) and (b) Lu metals from 300 to 2 K.

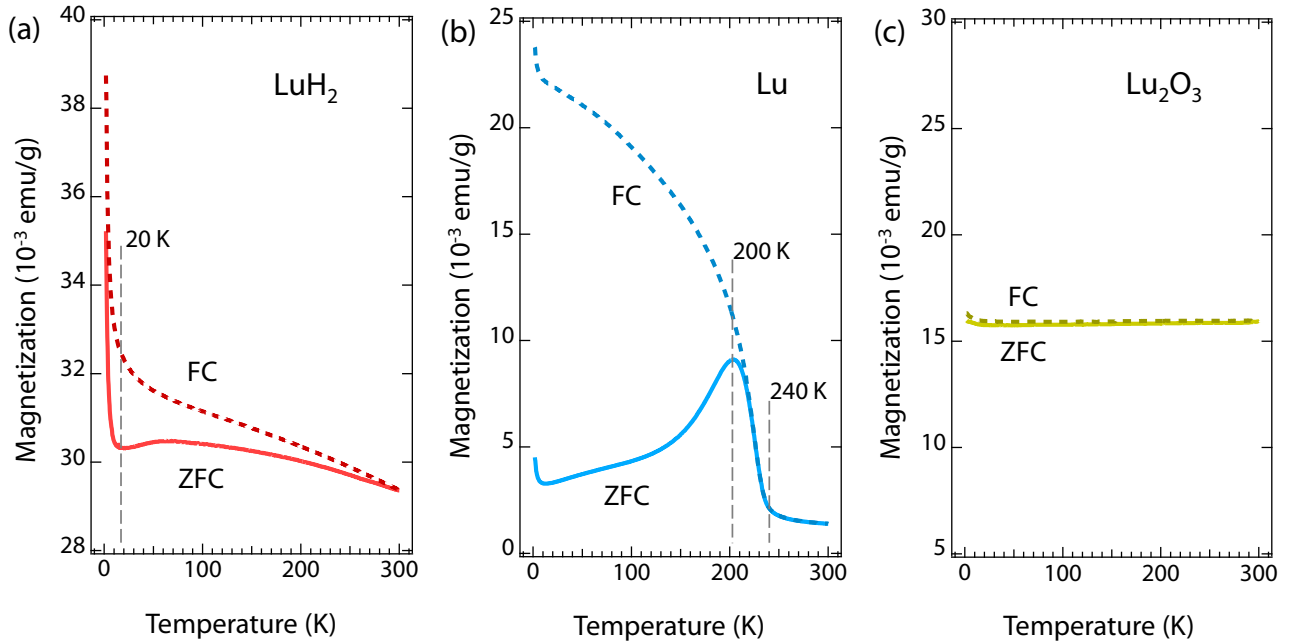


FIG. 4. Temperature-dependent magnetizations (ZFC and FC) of LuH₂ powders (compressed), Lu metals, and Lu₂O₃ powders from 300 to 2 K. During measurements, the cooling field was set at 1000 Oe.

III. RESULTS AND DISCUSSION

First, we explored the crystal structures of these three samples. As shown in Fig. 1, the diffraction peaks of these three samples are totally different. The dominative feature of LuH₂ XRD data (see the red curve in Fig. 1) is the four main diffraction peaks in the range 20-70 degrees, which agrees well with the previous report [4]. The crystal structure of LuH₂ is cubic (Fm $\bar{3}$ m

space group) with an estimated lattice parameter $a \sim 5.03\text{\AA}$. Also, it is noteworthy that several small peaks can be seen in the XRD curve of LuH₂. Compared to the XRD lineshapes of Lu and Lu₂O₃ (see blue and red curves in Fig. 1), it is indicated that the LuH₂ sample has little Lu and Lu₂O₃ compositions, which is consistent with the previous report [4].

To further investigate the chemical compositions of Lu, LuH₂, and Lu₂O₃ samples, we performed XPS at room temperature, which is a surface-sensitive technique to probe the valence states of compounds. As seen in Fig.2, apart from the oxygen (O 1s ~ 531 eV) and carbon (C 1s ~ 284.8 eV) existed on sample surfaces, no distinct impurities is detected, verifying the purity of these samples. Interestingly, a number of peaks can be observed in the XPS spectra, most of which are assigned to Lu core-level states such as Lu 4*f* (~ 9 eV), 5*p* (~ 28 eV), 4*d*_{5/2} (~ 196 eV), 4*d*_{3/2} (~ 207 eV), 4*p*_{3/2} (~ 360 eV), and 4*p*_{1/2} (~ 411 eV) states [17]. Here, we emphasize that the surfaces of both Lu and LuH₂ are easily oxidized.

Next, we characterized the electronic properties of Lu and LuH₂ samples by electrical transport from 300 to 2 K. As shown in Fig. 3, both Lu (size $\sim 3.7 \times 1.9 \times 0.5$ mm³) and LuH₂ (size $\sim 5.1 \times 6.1 \times 0.8$ mm³) are highly conducting, the resistances of which are ~ 10 Ω and $\sim 10^{-4}$ Ω , respectively. With decreasing the temperature from 300 to 2 K, the resistance of LuH₂ is almost independent of temperature, whereas the resistance of Lu shows a strong linear behavior down to 20 K, then becomes a constant below 20 K. The resistance of Lu changed from 5.13×10^{-4} Ω at 300 K to 0.1×10^{-4} Ω at 20 K. It is noted that the data in Fig. 3 (a) is noisy due to the measured LuH₂ sample in Fig. 3 (a) being a compressed tablet from LuH₂ powders.

At last, to investigate the magnetic properties of Lu, LuH₂, and Lu₂O₃, we measured the zero-field cooling (ZFC) and field cooling (FC) magnetization curves by SQUID. During measurements, the cooling field was set at 1000 Oe. As seen in Fig. 4, Lu, LuH₂, and Lu₂O₃ present totally different magnetic properties. For LuH₂, the magnetization under FC protocol (see the dashed red curve in Fig. 4(a)) increases monotonously with decreasing the temperature to 20 K, whereas the magnetization has a bump (~ 60 K) for the ZFC protocol (see the solid red curve in Fig. 4(a)). Comparing to LuH₂ in Fig. 4(a), unexpectedly, the behavior of temperature-dependent magnetization of Lu is more complicated. As shown in Fig. 4(b), there is a distinct separation between ZFC and FC curves, which can result from the spin-glass transition [18–20]. With decreasing the temperature from 300 to 2 K, two critical features (at ~ 240 K and ~ 200 K) can be observed. The first one ~ 240 K can be interpreted as the paramagnetic to the ferromagnetic phase transition, whereas the second one ~ 200 K is due to a spinglass transition. In contrast to Lu and LuH₂, the magnetizations of Lu₂O₃ are almost independent of temperature, indicating the diamagnetic nature of Lu₂O₃ [21].

IV. CONCLUSION

In this work, we characterized the electronic and magnetic properties of Lu, LuH₂, and Lu₂O₃ by XRD, XPS, electrical transport, and SQUID. Both Lu and LuH₂ are metallic, whereas Lu₂O₃ is insulating. The resistance of Lu has a linear behavior depending on temperature, whereas the the resistance of LuH₂ is almostly independent of temperature. More interestingly, the magnetization of both Lu and LuH₂ show a spinglass feature. Our work uncovered unexpected magnetic properties of Lu-based compounds.

V. ACKNOWLEDGMENTS

We thank Xinming Wang, Jie Sun, and Kemin Jiang for helping experimental setup. We acknowledge insightful discussions with Baomin Wang and Shaozhu Xiao. This work was supported by the National Key R&D Program of China (Grant No. 2022YFA1403000), the National Natural Science Foundation of China (Grant Nos. U2032126 and 11874058), the Pioneer

Hundred Talents Program of the Chinese Academy of Sciences, the Zhejiang Provincial Natural Science Foundation of China under Grant No. LXR22E020001, the Beijing National Laboratory for Condensed Matter Physics, the Ningbo Natural Science Foundation (Grant No. 20221JCGY010338), and the Ningbo Science and Technology Bureau (Grant No. 2022Z086).

-
- [1] N. Dasenbrock-Gammon Snider, E. McBride, R. Pasan, H. Durkee, D. Khalvashi-Sutter, N. Munasinghe, S. Dissanayake, S. E. Lawler, K. V. Salamat, A. Dias, R. P., Evidence of near-ambient superconductivity in a N-doped lutetium hydride, *Nature* **615**, 244 (2023).
- [2] Z. Li, X. He, C. Zhang, K. Lu, B. Bin, J. Zhang, S. Zhang, J. Zhao, L. Shi, and S. Feng, Superconductivity above 70 K experimentally discovered in lutetium polyhydride, arXiv:2303.05117 (2023).
- [3] M. Liu, X. Liu, J. Li, J. Liu, Y. Sun, X.-Q. Chen, and P. Liu, On parent structures of near-ambient nitrogen-doped lutetium hydride superconductor, arXiv:2303.06554 (2023).
- [4] P. Shan, N. Wang, X. Zheng, Q. Qiu, Y. Peng, and J. Cheng, Pressure-induced color change in the lutetium dihydride LuH₂, *Chinese Phys. Lett.* (2023).
- [5] X. Ming, Y.-J. Zhang, X. Zhu, Q. Li, C. He, Y. Liu, B. Zheng, H. Yang, and H.-H. Wen, Absence of near-ambient superconductivity in LuH_{2±x}N_y, arXiv:2303.08759 (2023).
- [6] H. Song, Z. Zhang, T. Cui, C. J. Pickard, V. Z. Kresin, and D. Duan, High T_c superconductivity in Heavy Rare Earth hydrides: correlation between the presence of the *f* states on the Fermi surface, nesting and the value of T_c, arXiv:2010.12225 (2020).
- [7] M. Du, H. Song, Z. Zhang, D. Duan, and T. Cui, Room-Temperature Superconductivity in Yb/Lu Substituted Clathrate Hexahydrides under Moderate Pressure, *Research* **2022**, 9784309 (2022).
- [8] M. Shao, S. Chen, W. Chen, K. Zhang, X. Huang, and T. Cui, Superconducting ScH₃ and LuH₃ at Megabar Pressures, *Inorg. Chem.* **60**, 15330 (2021).
- [9] D. Wang, Y. Ding, and H.-K. Mao, Future Study of Dense Superconducting Hydrides at High Pressure, *Materials* **14**, 7563 (2021).
- [10] K. Kaminaga, D. Oka, T. Hasegawa, and T. Fukumura, New Lutetium Oxide: Electrically Conducting Rock-Salt LuO Epitaxial Thin Film, *ACS omega* **3**, 12501 (2018).
- [11] G. N. Chesnut and Y. K. Vohra, Phase transformation in lutetium metal at 88 GPa, *Phys. Rev. B* **57**, 10221 (1998).
- [12] M. Tkacz and T. Palasyuk, Pressure induced phase transformation of REH₃, *J. Alloys Compd.* **446**, 593 (2007).
- [13] D. Zhang, W. Lin, Z. Lin, L. Jia, W. Zheng, and F. Huang, Lu₂O₃: A promising ultrawide bandgap semiconductor for deep UV photodetector, *Appl. Phys. Lett.* **118**, 211906 (2021).
- [14] S. Matsumoto and A. Ito, Chemical vapor deposition route to transparent thick films of Eu³⁺-doped HfO₂ and Lu₂O₃ for luminescent phosphors, *Opt. Mater. Express* **10**, 899 (2020).
- [15] R. S. Lee and S. Legvold, Hall Effect of Gadolinium, Lutetium, and Yttrium Single Crystals, *Phys. Rev.* **162**, 431 (1967).
- [16] F. H. Spedding and J. J. Croat, Magnetic properties of high purity yttrium, lanthanum, and lutetium and the effects of impurities on these properties, *J. Chem. Phys.* **59**, 2451 (1973).
- [17] V. V. Kaichev, T. I. Asanova, S. B. Erenburg, T. V. Perevalov, V. A. Shvets, and V. A. Gritsenko, Atomic and Electronic Structures of Lutetium Oxide Lu₂O₃, *J. Exp. Theor. Phys.* **116**, 323 (2013).
- [18] J. A. Mydosh, *Spin Glasses: An Experimental Introduction* (Taylor & Francis, London, 1993).
- [19] F. Wang, J. Kim, and Y. Kim, Spin-glass behavior in LuFe₂O_{4+δ}, *Phys. Rev. B* **80**, 024419 (2009).
- [20] W. Huang, X. Zhang, H. Du, R. Yang, Y. Tang, Y. Sun, and Z. Cheng, Intrinsic exchange bias effect in phase-separated La_{0.82}Sr_{0.18}CoO₃ single crystal, *J. Phys.: Condens. Matter* **20**, 445209 (2008).
- [21] L. Ben Farhata, M. Amamib, E.K. Hlil, and R. Ben Hassen, Synthesis, structure and magnetic properties of the Lu₂O₃-CoO mixed system, *Mater. Chem. Phys.* **123**, 737 (2010).